J|A|C|S
ARTICLES
Published on Web 11/23/2004

Design and Synthesis of Highly Sensitive and Selective Fluorescein-Derived Magnesium Fluorescent Probes and Application to Intracellular 3D Mg^{2+} Imaging

Hirokazu Komatsu,[†] Naoko Iwasawa,[‡] Daniel Citterio,[‡,§] Yoshio Suzuki,[‡,||] Takeshi Kubota,[⊥] Kentaro Tokuno,[⊥] Yoshiichiro Kitamura,[⊥] Kotaro Oka,[⊥] and Koji Suzuki*[,†,‡,||]

Contribution from the Departments of Applied Chemistry and of Biosciences and Informatics, Faculty of Science and Technology, Keio University, 3-14-1 Hiyoshi, Kohoku-ku, Yokohama, Kanagawa 223-8522, Japan, Kanagawa Academy of Science and Technology, KSP West, 3-2-1 Sakato, Kawasaki, Kanagawa 213-0012, Japan, and JST-CREST, 4-1-8 Honcho, Kawaguchi, Saitama 332-0012, Japan

Received January 22, 2004; Revised Manuscript Received October 8, 2004; E-mail: suzuki@applc.keio.ac.jp

Abstract: The role of intracellular magnesium ions is of high interest in the fields of pharmacology and cellular biology. To accomplish the dynamic and three-dimensional imaging of intracellular Mg^{2+}, there is a strong desire for the development of optimized Mg^{2+} fluorescent probes. In this paper we describe the design, synthesis, and cellular application of the three novel Mg^{2+} fluorescent probes KMG-101, -103, and -104. The compounds of this series feature a charged β-diketone as a binding site specific for Mg^{2+} and a fluorescein residue as the fluorophore that can be excited with an Ar^{+} laser such as is widely used in confocal scanning microscopy. This molecular design leads to an intensive off−on-type fluorescent response toward Mg^{2+} ions. The two fluorescent probes KMG-103 and -104 showed suitable dissociation constants ($K_{d,Mg^{2+}} = 2$ mM) and nearly a 10-fold fluorescence enhancement over the intracellular magnesium ion concentration range (0.1−6 mM), allowing high-contrast, sensitive, and selective Mg^{2+} measurements. For intracellular applications, the membrane-permeable probe KMG-104AM was synthesized and successfully incorporated into PC12 cells. Upon application of the mitochondria uncoupler FCCP to the probe-incorporated cells, the resulting increase in the free magnesium ion concentration could be followed over time. By using a confocal microscope, the intracellular 3D magnesium ion concentration distributions were satisfactorily observed.

Introduction

The magnesium ion is the most abundant divalent cation in cells, and intracellular magnesium ions play a critical role as enzyme cofactors in DNA synthesis[1] and protein phosphorylation.[2] Furthermore, they modulate signal transduction,[3] various transporters,[4] and ion channels,[5] and they are known to regulate phosphoinositide-derived second messengers.[6]

Recently, fluorescent probes have been widely used as tools for the dynamic measurement of ion distributions and concentrations in cells.[7] They are highly sensitive and offer imaging by fluorescent microscopy in an easier and less cell damaging way than other methods (e.g., ion-selective electrodes, NMR techniques). Many fluorescent probes for the measurement of Ca^{2+}, NO, Zn^{2+}, and alkali metals have been reported.[8] For Ca^{2+}, the commercially available Fura-2 and Fluo-3 are widely used.

Fluorescein-based fluorescent probes for intracellular applications have been developed for Ca^{2+}, NO, and Zn^{2+}.[8,9] Fluorescein is characterized by large extinction coefficients (90000 $M^{-1}cm^{-1}$), high quantum yields (0.95), water solubility, biological tolerance, and the ability to be excited by the widely

[†] Department of Applied Chemistry, Keio University.
[‡] Kanagawa Academy of Science and Technology.
[§] Present address: Center for Chemical Sensors and Chemical Information Technology (CCS), Swiss Federal Institute of Technology (ETH), Technoparkstrasse 1, CH-8005 Zurich, Switzerland.
[||] JST-CREST.
[⊥] Department of Biosciences and Informatics, Keio University.

(1) Hartwig, A. *Mutat. Res.* **2001**, *475* (1, 2), 113−121.
(2) O'Rourke, B.; Backx, P. H.; Marban, E. *Science* **1992**, *257*, 45−248.
(3) Politi, H. C.; Preston R. R. *Neuroreport* **2003**, *14* (5), 659−668.
(4) Kubota, T.; Tokuno, K.; Nakagawa, J.; Kitamura, Y.; Ogawa, H.; Suzuki, Y.; Suzuki, K.; Oka, K. *Biochem. Biophys. Res. Commun.* **2003**, *303*, 332−336.
(5) (a) Jóna, I.; Szegedi, C.; Sárközi, S.; Szentesi, P.; Csernoch, L.; Kovács, L. *Pfluegers Arch.* **2001**, *441*, 729−738. (b) Nadler, M. J. S.; Hermosura, M. C.; Inabe, K.; Perraud. A.; Zhu, Q.; Stokes, A. J.; Turosaki, T.; Kinet, J.; Penner, R.; Scharenberg, A. M.; Flelg, A. *Nature* **2001**, *411*, 590−595. (c) Schmitz, C.; Perraud, A.; Johnson, C. O.; Inabe, K.; Smith, M. K.; Penner, R.; Kurosaki, T.; Fleig, A.; Scharenberg, A. M. *Cell* **2003**, *113*, 191−200. (d) Kozak, J. A.; Cahalan, M. D. *Biophys. J.* **2003**, *84*, 922−927.
(6) (a) Leyssens, A.; Nowicky, A. V.; Patterson, L.; Crompton, M.; Duchen, M. R. *J. Physiol.* **1996**, *496.1*, 111−128. (b) Raftos, J. E.; Lew, V. L.; Flatman, P. W. *Eur. J. Biochem.* **1999** *263*, 635−645.
(7) Haugland, R. P. *Handbook of Fluorescent Probes and Research Chemicals*, 9th ed.; Molecular Probes: Eugene, OR, 2002.
(8) (a) Grynkiewicz, G.; Poenie, M.; Tsien, R. Y. *J. Biol. Chem.* **1985**, *260* (6), 3440−3450. (b) Kojima, H.; Nakatsubo, N.; Kikuchi, K.; Kawahara, S.; Kirino, Y.; Nagoshi, H.; Hirata, Y.; Nagano, T. *Anal. Chem.* **1998**, *70*, 2466. (c) Walkup, G. K.; Burdette, S. C.; Lippard, S. J.; Tsien, R. Y. *J. Am. Chem. Soc.* **2000**, *122*, 5644. (d) Minta, A.; Tsien, R. Y. *J. Biol. Chem.* **1989**, *264*, 19449−19457.

used 488 nm line of the Ar^+ laser as applied in confocal scanning microscopy. The excitation with visible light reduces cellular damage and autofluorescence.[10]

In contrast to the large variety of excellent Ca^{2+} fluorescent probes, there are few Mg^{2+} fluorescent probes that have satisfactory properties. In the development of magnesium fluorescent probes, first, FURAPTRA (Mag-Fura-2)[11] and several probes that have enhanced optical characteristics were reported,[7] but those having an APTRA (*O*-aminophenol-*N*,*N*,*O*-triacetic acid) binding site suffer from the lack of selectivity as they bind to Ca^{2+} 100-fold stronger than to Mg^{2+}, resulting in a strong Ca^{2+} interference.[12]

We previously reported KMG-20AM[13] as having a charged β-diketone binding site and a coumarin fluorophore that has a strongly improved magnesium selectivity. However, this intramolecular charge transfer (ICT) type probe had a relatively low affinity for intracellular magnesium ($K_{d,Mg^{2+}}$ = 10 mM) and low sensitivity. Additionally, it is not excitable by the Ar^+ laser commonly used with a confocal microscope. Park and coworkers developed Mg^{2+}-sensitive nanoparticles for intracellular use (PEBBLEs).[22] They reported the particles to be stable and show affinities and spectroscopic limitations similar to those of KMG-20AM, since they are based on the same dye structure. The fluorescein derivative 2′-CF[14] developed in cooperation with Nagano was applicable with the confocal microscope, but it showed a lower affinity for magnesium ($K_{d,Mg^{2+}}$ is near 10 mM) and suffered from pH interference. Moreover, the range of the intracellular magnesium concentration changes is smaller (0.1−6 mM) than for calcium concentrations (100 nM to 1 mM), thus requiring high sensitivity, selectivity, and suitable affinity of Mg^{2+} fluorescent probes.

In this paper we describe the design, synthesis, and application of the excellent magnesium-selective fluorescent probes KMG-101, -103, and −104, which fulfill the important requirements as outlined above. They have a fluorescein residue as the fluorophore and are aimed to show the highly sensitive photoinduced electron transfer-type (PET) response and varying Mg^{2+} affinities and allow Ar^+ laser excitation. The fluorescence response of the compounds in this KMG-100 series toward Mg^{2+}, other alkali-metal and alkaline-earth-metal ions, and pH was measured and compared.

Additionally, KMG-104AM, the membrane-permeable ester-modified[15] derivative of KMG-104, which showed the best properties among the members of the KMG-100 series, was synthesized. The permeation of KMG-104AM through the cell membrane of PC12 cells was demonstrated, and the FCCP-induced magnesium ion concentration response was followed.

Scheme 1. Synthesis of KMG-101

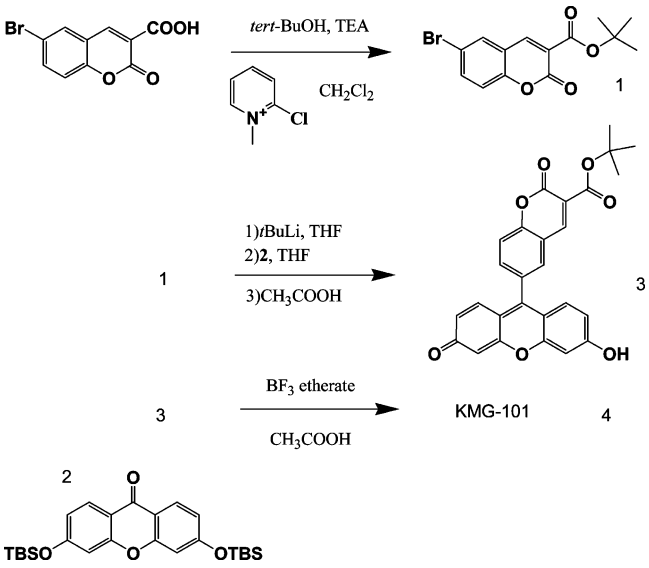

By using a confocal microscope, the 3D distribution of Mg^{2+} in PC12 cells was observed.

Experimental Section

Synthesis. General Procedures. All starting materials and reagents were purchased from Tokyo Kasei Kogyo (Tokyo, Japan) or Aldrich Chemical (Milwaukee, WI). THF was distilled over sodium benzophenone ketyl, and CH_2Cl_2 was distilled over $CaCl_2$. All other solvents, purchased from Aldrich, were GR grade or dry grade and used without further purification. 3,6-Bis(*tert*-butyldimethylsilanyloxy)xanthen-9-one was synthesized according to the report by Grover et al.[16] 1-Formyl-4-oxo-4*H*-quinolizine-3-carboxylic acid ethyl ester was synthesized as reported by Levy et al.[17] 4-Fluorobenzene-1,3-diol was synthesized according to Sun et al.[10]

The ^1H NMR spectra were recorded using a JEOL JNM-LA300 spectrometer in $CDCl_3$ or CD_3OD. Coupling constants are given in hertz, and all chemical shifts are relative to the internal standard of tetramethylsilane. The ESI-MS spectra were recorded on a PerSeptive Biosystems Mariner spectrometer with MeOH as the eluent. All air- or moisture-sensitive reactions were carried out in oven-dried glassware under an argon atmosphere with magnetic stirring.

Synthesis of KMG-101. (a) 6-Bromo-2-oxo-2*H*-chromene-3-carbocylic Acid *tert*-Butyl Ester. See Scheme 1 for an illustration of the synthesis of KMG-101. To a solution of 6-bromo-2-oxo-2*H*-chromene-3-carboxylic acid (2.09 g, 7.76 mmol, 1 equiv) in 20 mL of CH_2Cl_2 were added *tert*-butyl alcohol (0.654 g, 8.82 mmol, 1.14 equiv) and 3 mL of triethylamine. A solution of 2-chloro-*N*-methylpyridinium iodide (3.92 g, 15.34 mmol, 1.97 equiv) dissolved in 45 mL of CH_2Cl_2 was then dropwise added. The resulting solution was refluxed for 24 h. After being cooled to room temperature, the reaction mixture was diluted with CH_2Cl_2, washed with water, saturated aqueous $NaHCO_3$ solution, and brine, dried over Na_2SO_4, filtered, and concentrated by evaporation of the solvent. The crude product was purified by silica gel column chromatography (CH_2Cl_2/MeOH = 100/1 v/v). It was further purified by recrystallization from EtOAc to give 6-bromo-2-oxo-2*H*-chromene-3-carbocylic acid *tert*-butyl ester as a white solid (1.40 g, 6.00 mmol, 55.3%): ^1H NMR (300 MHz, $CDCl_3$) δ 1.60 (s, 9H), 7.24 (d, 1H, 8.8 Hz), 7.70 (d, 1H, 8.8 Hz), 7.74 (s, 1H), 8.30 (s, 1H).

(9) Minta, J. P.; Kao, Y.; Tsien, R. Y. *J. Biol. Chem.* **1989**, *264*, 8171. (b) Hirano, T.; Kikuchi, K.; Urano, Y.; Higuchi, T.; Nagano, T. *J. Am. Chem. Soc.* **2000**, *122*, 12399-12400. (c) Hirano, T.; Kikuchi, K.; Urano, Y.; Nagano, T. *J. Am. Chem. Soc.* **2002**, *124*, 6555−6562.
(10) Sun, W.; Gee, K. R.; Klaubert, D. H.; Haugland, R. P. *J. Org. Chem.* **1997**, *62*, 6469−6475.
(11) Raju, B.; Murphy, E.; Levy, L. A.; Hall, R. D.; London, R. E. *Am. J. Physiol.* **1989**, *256*, C540−C548.
(12) Pesco, J.; Salmon, J.; Vigo, J.; Viallet, P. *Anal. Biochem.* **2001**, *290*, 221−231.
(13) (a) Suzuki, Y.; Komatsu, H.; Ikeda, T.; Saito, N.; Araki, S.; Citterio, D.; Hisamoto, H.; Kitamura, Y.; Kubota, T.; Nakagawa, J.; Oka, K.; Suzuki, K. *Anal. Chem.* **2002**, *74* (6), 1423−1428. (b) Suzuki, K.; Suzuki, Y.; Oka, K. PCT Int. Appl. WO 0212867, 2002.
(14) Shoda, T.; Kikuchi, K.; Kojima, H.; Urano, Y.; Komatsu, H.; Suzuki, K.; Nagano, T. *Analyst* **2003**, *128*, 719−723.
(15) (a) Ferres, H. *Chem. Ind.* **1980**, 435−440. (b) Tsien, R. Y. *Nature* **1981**, *290*, 527−528. (c) Thomas, J. A.; Buchsbaum, R. N.; Zimniak, A.; Racker, E. *Biochemistry* **1979**, *18* (11), 2210−2218.
(16) Grover, P. K.; Shah, G. D.; Shah, R. C. *J. Indian Chem. Soc.* **1955**, 3982−3985.
(17) Otten, P. A.; London, R. E.; Levy, L. A. *Bioconjugate Chem.* **2001**, *12*, 203-212.

Scheme 2. Synthesis of KMG-103 and -104

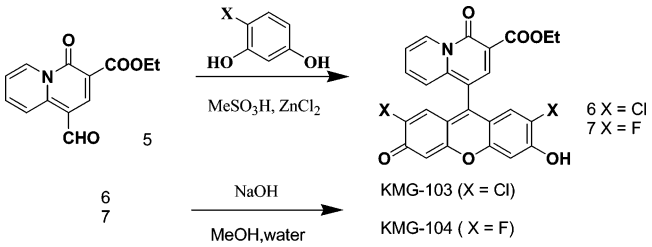

(b) 6-(6-Hydroxy-3-oxo-3*H*-xanthen-9-yl)-2-oxo-2*H*-chromane-3-carboxylic Acid *tert*-Butyl Ester. 6-Bromo-2-oxo-2*H*-chromene-3-carboxylic acid *tert*-butyl ester (604 mg, 1.86 mmol, 1 equiv) was dissolved in 45 mL of THF and cooled in an ether/dry ice bath (−100 °C). *tert*-Butyllithium (2.2 mL, 2 equiv, 1.7 M solution in pentane) was added, and the mixture was stirred for 1.5 h, resulting in an orange-colored solution. To this solution was slowly added via a syringe 3,6-bis(*tert*-butyldimethylsilanyloxy)xanthen-9-one (1.85 g, 4.05 mmol, 2.18 equiv) dissolved in 30 mL of THF. After being stirred for 5 h, the reaction was quenched by adding water and THF. The reaction mixture was dissolved in EtOAc, washed with water, saturated aqueous $NaHCO_3$ and brine, dried over Na_2SO_4, filtered, and concentrated by evaporation of the solvent. The residue was dissolved in 10 mL of AcOH, stirred for 1 h, and concentrated. The crude mixture was then purified by silica gel column chromatography (CH_2Cl_2/MeOH/AcOH = 100/5/1). Further purification was performed by preparative TLC (Merck) (CH_2Cl_2/MeOH/AcOH = 100/10/1) to give 6-(6-hydroxy-3-oxo-3*H*-xanthen-9-yl)-2-oxo-2*H*-chromane-3-carboxylic acid *tert*-butyl ester as an orange solid (85.6 mg, 0.19 mmol, 10.1%): ^{1}H NMR (300 MHz, CD_3OD) δ 1.30 (s, 1H), 6.68−7.72 (m, 4H), 7.22 (d, 2H, 9.5 Hz), 7.63 (d, 1H, 8.5 Hz), 7.77 (d, 1H, 8.5 Hz), 7.92 (s, 1H), 8.69 (s, 1H).

(c) 6-(6-Hydroxy-3-oxo-3*H*-xanthen-9-yl)-2-oxo-2*H*-chromane-3-carboxylic Acid (KMG-101). To a solution of 6-(6-hydroxy-3-oxoxanthen-9-yl)-2-oxo-2*H*-chromene-3-carboxylic acid *tert*-butyl ester (25 mg, 0.05 mmol, 1 equiv) in 5 mL of AcOH was added 0.5 mL of trifluoroborane etherate, and the solution was then stirred for 6 h at room temperature. The reaction was stopped by adding water, and the mixture was concentrated. It was then dissolved in aqueous $NaHCO_3$ and washed twice with EtOAc and hexane. The aqueous phase was acidified with HCl and cooled to −10 °C to allow the formation of a precipitate, to give 6-(6-hydroxy-3-oxo-3*H*-xanthen-9-yl)-2-oxo-2*H*-chromane-3-carboxylic acid as an orange solid (8.8 mg, 0.02 mmol, 40.1%): ^{1}H NMR (300 MHz, CD_3OD) δ 7.30 (d, 2H, 9.3 Hz), 7.42 (s, 2H), 7.76 (d, 1H, 8.5 Hz), 7.85 (d, 2H, 9.3 Hz), 7.94 (d, 1H, 8.5 Hz), 8.10 (s, 1H), 8.90 (s, 1H); ESI-MS *m*/*z* 401.1 ($M - H^+$). The quantum yield of the KMG-101−Mg^{2+} complex (10 μM KMG-101, 50 mM HEPES, 130 mM KCl, 20 mM NaCl, 100 mM $MgCl_2$, pH 7.2) was 0.2 as determined with 10 μM fluorescein (50 mM phosphate buffer, pH 9) used as the standard (0.92).[10]

Synthesis of KMG-103. (a) 1-(2,7-Dichloro-6-hydroxy-3-oxo-3*H*-xanthen-9-yl)-4-oxo-4*H*-quinolizine-3-carboxylic Acid Ethyl Ester. See Scheme 2 for an illustration of the synthesis of KMG-103. 1-Formyl-4-oxo-4*H*-quinolizine-3-carboxylic acid ethyl ester (1.60 g, 6.52 mmol, 1 equiv) and 4-chlororesorcinol (2.17 g, 15.0 mmol, 2.30 equiv) were dissolved in 100 mL of $MeSO_3H$. $ZnCl_2$ (10.0 g, 73.4 mmol, 11.2 equiv) was then added, and the solution was stirred for 2 h at 80 °C. After the solution was cooled to room temperature, water was added, and the product was extracted twice with chloroform. The combined organic layers were washed with water and brine, dried over Na_2SO_4, filtered, and concentrated. The crude product was purified by column chromatography on silica gel (CH_2Cl_2/MeOH/AcOH = 10/1/0 to 10/1/0.1), followed by further purification using preparative TLC (CH_2Cl_2/MeOH/AcOH = 10/1/0.1), and recrystallization from EtOAc to give 1-(2,7-dichloro-6-hydroxy-3-oxo-3*H*-xanthen-9-yl)-4-oxo-4*H*-quinolizine-3-carboxylic acid ethyl ester as a red solid (159 mg, 0.32 mmol, 4.91%): ^{1}H NMR (300 MHz, $CDCl_3$) δ 1.31 (t, 3H, 6.9 Hz), 4.29 (q, 2H, 7.2 Hz), 6.63 (s, 2H), 7.22 (s, 2H), 7.44 (d, 1H, 8.7 Hz), 7.49−7.54 (m, 1H), 7.80−7.85 (m, 1H), 8.35 (s, 1H), 9.57 (d, 1H, 6.6 Hz); ESI-MS *m*/*z* 496.0 (M^-).

(b) 1-(2,7-Dichloro-6-hydroxy-3-oxo-3*H*-xanthen-9-yl)-4-oxoquinolizine-3-Carboxylic Acid (KMG-103). To a solution of 1-(2,7-dichloro-6-hydroxy-3-oxo-3*H*-xanthen-9-yl)-4-oxo-4*H*-quinolizine-3-carboxylic acid ethyl ester (20 mg, 0.04 mmol, 1 equiv) in 4 mL of MeOH was added 1 mL of 3 M NaOH, and the solution was stirred for 2 days at room temperature. Water was added to the mixture and then washed twice with EtOAc−hexane. The aqueous phase was acidified with HCl and cooled to −10 °C to allow the precipitation of 1-(2,7-dichloro-6-hydroxy-3-oxo-3*H*-xanthen-9-yl)-4-oxoquinolizine-3-carboxylic acid as an orange-red solid (5 mg, 0.01 mmol, 26%): ^{1}H NMR (300 MHz, CD_3OD) δ 6.90 (s, 2H), 7.48 (s, 2H), 7.55 (d, 1H, 12.3 Hz), 7.65−7.70 (m, 1H), 7.90−7.95 (m, 1H), 8.45 (s, 1H), 9.60 (d, 1H, 7.5 Hz); ESI-MS *m*/*z* 466.2 (M^-). The quantum yield of the KMG-103−Mg^{2+} complex (5 μM KMG-103, 50 mM HEPES, 130 mM KCl, 20 mM NaCl, 100 mM $MgCl_2$ pH 7.2) was 0.02 as determined with 10 μM fluorescein (50 mM phosphate buffer, pH 9) used as the standard (0.92).

Synthesis of KMG-104. (a) 1-(2,7-Difluoro-6-hydroxy-3-oxo-3*H*-xanthen-9-yl)-4-oxo-4*H*-quinolizine-3-carboxylic Acid Ethyl Ester. 1-Formyl-4-oxo-4*H*-quinolizine-3-carboxylic acid ethyl ester (300 mg, 1.22 mmol, 1 equiv) and 4-fluorobenzene-1,3-diol (430 mg, 3.36 mmol, 2.74 equiv) were dissolved in 20 mL of $MeSO_3H$. $ZnCl_2$ (2 g, 14.67 mmol, 12 equiv) was then added, and the solution was stirred for 2 h at 80 °C. After the solution was cooled to room temperature, water was added, and the mixture was extracted twice with chloroform. The combined organic layers were washed with water and brine, dried over Na_2SO_4, filtered, and concentrated. The crude product was purified by column chromatography on silica gel (CH_2Cl_2/MeOH/AcOH = 10/1/0 to 10/1/0.1), followed by further purification using preparative TLC (CH_2Cl_2/MeOH/AcOH = 10/1/0.1), and recrystallization from EtOAc to give 1-(2,7-difluoro-6-hydroxy-3-oxo-3*H*-xanthen-9-yl)-4-oxo-4*H*-quinolizine-3-carbox ylic acid ethyl ester as a red solid (49 mg, 0.11 mmol, 8.64%): ^{1}H NMR (300 MHz, CD_3OD) δ 1.31 (t, 3H, 6.9 Hz), 4.30 (q, 2H, 7.1 Hz), 6.35−6.45 (m, 2H), 6.85−7.0 (m, 2H), 7.30−7.50 (m, 2H), 7.75−7.85 (m, 1H), 8.28 (s, 1H), 9.50 (d, 1H, 6.6 Hz); ESI-MS *m*/*z* 462.3 (M^-).

(b) 1-(2,7-Difluoro-6-hydroxy-3-oxo-3*H*-xanthen-9-yl)-4-oxo-4*H*-quinolizine-3-carboxylic Acid (KMG-104). To a solution of 1-(2,7-difluoro-6-hydroxy-3-oxo-3*H*-xanthen-9-yl)-4-oxo-4*H*-quinolizine-3-carboxylic acid ethyl ester (17.5 mg, 0.38 mmol, 1 equiv) in 16 mL of MeOH was added 4 mL of 3 M NaOH was added, and the solution was stirred for 2 days at room temperature. Water was added to the mixture, and it was washed twice with EtOAc−hexane. The aqueous phase was acidified with HCl and cooled to −10 °C to allow the formation of a precipitate to give 1-(2,7-difluoro-6-hydroxy-3-oxo-3*H*-xanthen-9-yl)-4-oxo-4*H*-quinolizine-3-carboxylic acid as an orange-red solid (11 mg, 0.03 mmol, 66.8%). Further purification was performed by recrystallization from EtOAc and using an LIC-918 recycling preparative high-performance liquid chromatograph (Japan Analytical Industry Co., Ltd.) equipped with a YMC-pack ODS-A column with MeOH containing 0.2% (v/v) acetic acid as the eluent: ^{1}H NMR (300 MHz, CD_3OD) δ 6.78−6.80 (m, 2H), 6.98−7.02 (m, 2H), 7.51−7.68 (m, 2H), 7.85−7.95 (m, 1H), 8.43 (s, 1H), 9.57 (d, 1H, 7.5 Hz); ESI-MS *m*/*z* 434.3 (M^-), 436.1 ($M-H^+$). The quantum yield of the KMG-104−Mg^{2+} complex (5 μM KMG-104, 50 mM HEPES, 130 mM KCl, 20 mM NaCl, 100 mM $MgCl_2$, pH 7.2) was 0.02 as determined with 10 μM fluorescein (50 mM phosphate buffer, pH 9) used as the standard (0.92). The ^{1}H NMR spectrum of KMG-104 is shown in the Supporting Information.

1-(6-Acetoxy-2,7-difluoro-3-oxo-3*H*-xanthen-9-yl)-4-oxo-4*H*-quinolizine-3-carboxylic Acid Acetoxymethyl Ester (KMG-104AM). To a solution of KMG-104 (1 equiv) in 4 mL of pyridine was added 2 mL

of Ac_2O, and the solution was stirred for 1 day at room temperature. Water was added to the mixture, and it was extracted twice with EtOAc. The combined organic layers were washed with water and brine, dried over Na_2SO_4, filtered, and concentrated. The acetylated product was then dissolved in 5 mL of CH_2Cl_2, 6 equiv of diisopropylethylamine and 5 equiv of AMBr (acetoxymethyl bromide) were added, and the solution was stirred for 1 day. Water was added to the mixture, and it was extracted twice with EtOAc. The combined organic layers were washed with water and brine, dried over Na_2SO_4, filtered, and concentrated. The crude product was purified by silica gel column chromatography on silica gel (CH_2Cl_2/MeOH = 10/1) to give 1-(6-acetoxy-2,7-difluoro-3-oxo-3*H*-xanthen-9-yl)-4-oxo-4*H*-quinolizine-3-carboxylic acid acetoxymethyl ester as an orange solid: ^{1}H NMR (300 MHz, $CDCl_3$) δ 2.01 (s, 2H), 2.08 (s, 3H), 6.03 (s, 2H), 6.62−6.72 (m, 2H), 6.91−6.95 (m, 2H), 7.43 (m, 1H), 7.52−7.55 (m, 1H), 7.69−7.73 (m, 2H), 8.33 (s, 1H), 9.63 (m, 1H).

UV−Vis and Fluorescence Spectroscopy. The fluorescent probes were dissolved in buffer solution (50 mM HEPES, 130 mM KCl, 20 mM NaCl, pH 7.2). All salts ($MgCl_2$·$6H_2O$, $CaCl_2$·$2H_2O$, KCl, NaCl) were of the highest purity available as purchased from KANTO. All absorption spectra were recorded using a Hitachi U-2001 double-beam spectrophotometer (Hitachi, Tokyo, Japan) with a 1 cm standard quartz cell. Fluorescence spectra in vitro were recorded on a Hitachi F-4500 fluorescence spectrophotometer or a Molecular device SPECTRAMAX GEMINI XS fluorescence microplate reader.

Measurement of pH Response. Good's buffer, MES (50 mM) for pH 5.0, 5.5, 6.0 and 6.5, and HEPES (50 mM) for pH 7.0, 7.5, 8.0, and 8.5 were selected, and the ionic strength was adjusted with 100 mM KCl. The concentration of the stock solution of each dye was 10^{-4} M (DMSO/water = 1/10), and it was diluted with the buffer to give the final concentrations. For measuring the pH response of the Mg^{2+} complex, $MgCl_2$ was added as a 100 mM solution.

Determination of Apparent Dissociation Constants for Mg^{2+} and Ca^{2+}. To determine the dissociation constant (K_d), the fluorescence intensity (F) was measured and fitted to the following equation:

$$F = F_{min} + (F_{max} - F_{min})[M]/(K_d + [M]) \quad (1)$$

$$\log((F - F_{min})/(F_{max} - F)) = \log [M] - \log K_d \quad (2)$$

where F_{max} is the maximum fluorescence intensity, F_{min} is the minimum fluorescence intensity, and [M] is the concentration of the metal ion.

When F_{max} was not experimentally accessible (KMG-101), the Benesi−Hildebrand plot method was used to determine K_d.

Chemical Reagents for the in Vivo Experiment. Dulbecco's modified Eagle's medium (DMEM), horse serum (HS), and fetal bovine serum (FBS) were purchased from GIBCO (Maryland). Nerve growth factor (NGF), carbonyl cyanide *p*-(trifluoromethoxy)phenylhydrazone (FCCP), and other reagents were obtained from Sigma (Missouri).

Cell Culture. PC12 cells were obtained from the RIKEN Tsukuba Institute, and were cultured at 37 °C in DMEM containing heat-inactivated serum (10% HS and 5% FBS, 25 U/mL penicillin, and 25 μg/mL streptomycin), under a humidified atmosphere containing 5% CO_2. For experimental use, the cells were cultured on glass cover slips coated with poly-D-lysine (PDL) and differentiated by culturing with 50 ng/mL NGF containing serum-free medium for 3 days.

Fluorescent Measurements and Analysis in Vivo. KMG-104AM was stored below 0 °C as a 10 mM stock solution in DMSO. Cells were incubated with 10 μM KMG-104AM in the culture medium for 30 min at 37 °C and then washed twice with a recording (normal) solution containing 125 mM NaCl, 5 mM KCl, 1.2 mM $MgSO_4$, 2 mM $CaCl_2$, 1.2 mM KH_2PO_4, 6 mM glucose, and 25 mM HEPES (pH 7.4), followed by a further incubation for 15 min to allow complete hydrolysis of the ester form of the KMG-104AM loaded into the cells.

Fluorescence images were acquired using an inverted microscope (ECLIPSE TE300 Nikon) equipped with a 40× (S Fluor, Nikon) objective, a 505 dichroic mirror, and a 535/55 barrier filter. A 150 W Xe lamp with a monochromator unit was used for the 480 nm excitation, and the fluorescence was measured with a CCD camera (HiSCA, Hamamatsu Photonics).

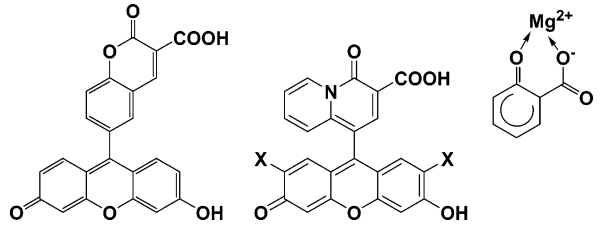

Figure 1. Chemical structures of the Mg^{2+} fluorescent probes KMG-101 (left), KMG-103 (center; X = Cl), and KMG-104 (center; X = F) and the charged β-diketone binding site (right).

3D images were acquired using a confocal scanning microscope mounted on a microscope (ECLIPSE E600FN, Nikon) equipped with a 60× (Plan Apo 60×, Nikon) objective and a 500 DM 500 LP optical filter. The 488 nm line of an argon ion laser was used for excitation, and the fluorescence was scanned using a confocal scanner unit (CSU21, YOKOGAWA), measured with a CCD camera ORCA-ER (Hamamatsu Photonics).

Calibration of KMG-104 in PC12 Cells. A total of 80 PC12 cells were incubated in a 10 μM KMG-104AM containing calibration solution (0 or 100 mM Mg^{2+} and 50 μM calcimycin) for 3 h. The fluorescence intensity of the resulting KMG-104AM-loaded cells was then measured by the same procedure as described above to determine the F_{max} and F_{min} values in the PC12 cells. Using these values for F_{max}, F_{min}, and K_d, the intracellular Mg^{2+} concentration in resting cells was determined according to eq 1.

Results and Discussion

Molecular Design. Figure 1 shows the molecular structures of the newly designed fluorescent probes KMG-101, -103, and −104. A charged β-diketone Mg^{2+}-selective binding site[13] was attached to the 9′-position of xanthene to induce a PET-type response.[18] However, a conventional PET-type response is based on the quenching of the fluorescence emission by the lone pair of a nitrogen donor and the ion-binding-induced inhibition of the quenching by the binding site HOMO-level relaxation (electron-withdrawing effect). In the case of the Mg^{2+}-selective binding site, a lone pair from an oxygen atom is involved instead of a nitrogen donor lone pair.

According to the HOMO-level PET theory,[19] the change in the HOMO level of the switching moiety with complexation to magnesium is relevant. Therefore, a decarboxylated fluorescein was used to lower the HOMO level of the binding site. At the same time, this leads to a decrease in the pK_a of the probe.[23] Furthermore, in the design of KMG-103 and -104, a halogen-substituted fluorescein was used to suppress the pH sensitivity, and a fluorine-substituted fluorescein was used to increase the photostability.[10] On the basis of the molecular design concepts, the probes KMG-101, -103, and -104 were synthesized.

(18) de Silva A. P.; Guanaratne, H. Q. N.; Gunnlaugsson, T.; Huxley, A. J. M.; McCoy, C. P.; Rademacher, J. T.; Rice, T. E. *Chem. Rev.* **1997**, *97*, 1515−1566.
(19) Nagano, T.; Yoshimura, T. *Chem. Rev.* **2002**, *102*, 1235−1269.
(20) (a) Quamme, G. A.; Dai, L.; Rabkin, S. W. *Am. J. Physiol.* **1993**, *265*, H281−288. (b) Cheng, C.; Reynolds. I. J. *Neuroscience* **2000**, *95* (4), 973−979. (c) Kato, H.; Gotoh, H.; Kajikawa, M.; Suto, K. *Brain Res.* **1997**, *779*, 329−333.
(21) Günther, T. *Magnesium* **1986**, *5*, 53−59.
(22) Park, E. J.; Brasuel, M.; Martin, A. P.; Kopelman, R. *Anal. Chem.* **2003**, *75*, 3784−3791.
(23) Martin, M. M.; Lindqvist. *J. Lumin.* **1975**, *10*, 381−390.

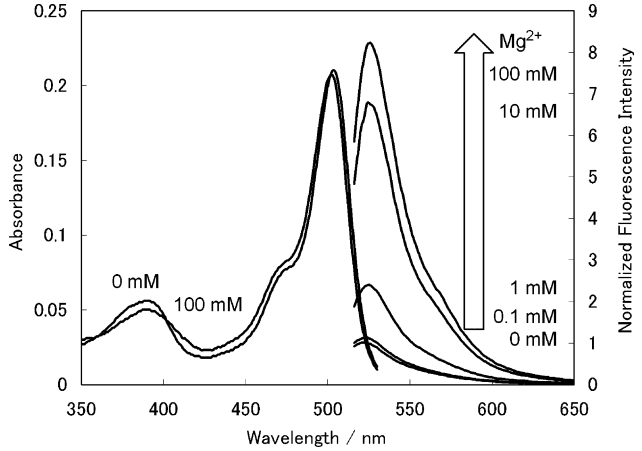

Figure 2. Absorbance and fluorescence emission spectra (excitation at 490 nm) of KMG-104 (5 μM) in the presence of various concentrations of Mg^{2+} ions (absorbance for $[Mg^{2+}] = 0$ mM and 100 mM, fluorescence for $[Mg^{2+}] = 0$, 0.1, 1, 10 and 100 mM, respectively). All spectra were measured at pH 7.20 (50 mM HEPES buffer, 130 mM KCl, 20 mM NaCl).

To enhance the cell membrane permeability during cell loading of the probe, the phenolic OH residue was converted to an acetyl group, and the carboxyl group to an acetoxymethyl group that is hydrolyzed by the intracellular esterase after membrane permeation, resulting in the regeneration of the free binding site of the probe.

Synthesis of the KMG-100 Derivatives. (a) KMG-101. The used starting material is a commercially available coumarin derivative, protected by a *tert*-butyl ester. The fluorescein synthesis by means of C−C bond formation was first reported by Tsien and co-workers.[9a] In this case, the moisture and temperature control are critical factors, and the reaction was performed at −100 °C with a dye yield of 10%. Finally, including the deprotection of the carboxyl group, KMG-101 was synthesized in six steps.

(b) KMG-103 and -104. The synthesis route based on the C−C bond formation as used for KMG-101 was not successful due to the low solubility of bromoquinolizine in THF. Furthermore, whereas the aldehyde derivative based condensation with resorcinol in $MeSO_3H$ succeeded, the subsequent oxidation step was not successful with either DDQ or chloranil. As an alternative, the one-pot synthesis of fluorescein based on the condensation of an aldehyde derivative with resorcinol, followed by oxidation and dehydration with $ZnCl_2$, was performed, yielding 10% of the dye. Finally, including the deprotection of the carboxyl group, KMG-103 was synthesized in four steps and KMG-104 in seven steps.

Fluorescence Properties. The absorbance and the fluorescence emission spectra of the compounds belonging to the KMG-100 series were recorded at a probe concentration of 5 μM in HEPES-buffered solutions (pH 7.2) with a biological ion background. A representative example is shown in Figure 2 for the magnesium-selective probe KMG-104. The optical properties in terms of the Mg^{2+} response are summarized in Tables 1 and 2.

For all the investigated probes, KMG-101, -103, and -104, the fluorescence emission intensity increased with increasing magnesium ion concentrations, while the absorption spectra showed only minor changes. The wavelengths of the maximum absorbance were slightly different among the probes, with the most bathochromic absorption observed for KMG-103 (515 nm)

Table 1. Comparison of the Optical Properties of Compounds in the KMG-100 Series[a]

compound	λ_{max}/nm (absorbance)	ϵ/(M^{-1} cm^{-1}) at λ_{max}	λ_{max}/nm (emission)
KMG-101	492	52000	519
KMG-101−Mg^{2+}	493	49000	516
KMG-103	515	38000	533
KMG-103−Mg^{2+}	517	39000	533
KMG-104	502	41000	523
KMG-104−Mg^{2+}	504	42000	523

[a] All data were obtained at pH 7.20 (50 mM HEPES buffer, 130 mM KCl, 20 mM NaCl). ϵ stands for the extinction coefficient (M^{-1} cm^{-1}). "−Mg^{2+}" indicates the Mg^{2+} complex (presence of 100 mM Mg^{2+} for KMG-103 and -104 and 500 mM for KMG-101).

Table 2. Comparison of the Sensitivity in the Presence of Mg^{2+} and Ca^{2+} Ions[a]

	$K_{d,Mg^{2+}}$/ mM	FEF for Mg^{2+}	$K_{d,Ca^{2+}}$/ mM	FEF for Ca^{2+}
KMG-101	100	2.73	150	1.58
KMG-103	1.8	11.1	6.3	1.88
KMG-104	2.1	8.18	7.5	1.61

[a] All data were obtained at pH 7.20 (50 mM HEPES buffer, 130 mM KCl, 20 mM NaCl). FEF stands for the fluorescence enhancement factor between an ion-free sample solution and a sample containing a 100 mM (500 mM for KMG-101) concentration of the respective cation.

and the most hypsochromic absorption for KMG-101 (492 nm). KMG-104 showed an intermediate λ_{max} value (504 nm). Both KMG-101 and -104 have the advantage of being excitable with the 488 nm line of the Ar^+ laser, while KMG-103 is preferably excited by the 514 nm line.

KMG-103 showed an 11.1-fold enhancement of the fluorescence emission intensity in the presence of 100 mM Mg^{2+}. Accordingly, an 8.18-fold enhancement was observed for KMG-104, and 2.73-fold for KMG-101. This observed type of response, characterized by fluorescence enhancement and basically unchanged absorbance resulting from the complexation to a cation, is usually called a PET (photoinduced electron transfer) type response. It is assumed to be controlled by the HOMO level of the switching moiety attached to the fluorescein. It was postulated that the presence of Mg^{2+} at the binding site inhibits the fluorescence suppression by PET. The N-substituted ring systems of KMG-103 and -104 showed lower baseline fluorescence intensities in the absence of magnesium ions compared to the probe KMG-101 with an O-donor. This observation can be explained by the higher HOMO levels in the case of KMG-103 and -104 (stronger electron donation by the nitrogen center), resulting in a more efficient photoinduced electron transfer in the absence of magnesium and relatively stronger fluorescence increase upon magnesium binding compared to those of KMG-101.

These observed spectral properties are consistent with the applied strategy for the molecular design of the probes, aiming at Ar^+ laser excitation, a decrease of intracellular autofluorescence, and a highly sensitive off−on-type response.

Mg^{2+} Affinity. The binding affinities of the indicators to the respective ions are reflected in the dissociation constants K_d. Because the intracellular magnesium concentration is in the range of 0.1−6 mM, the ideal dissociation constant for the Mg^{2+} fluorescent probes should be around 1 mM to make full use of the dynamic response range. The dissociation constants for Mg^{2+} ($K_{d,Mg^{2+}}$) were determined by a double-logarithmic plot[8a] as

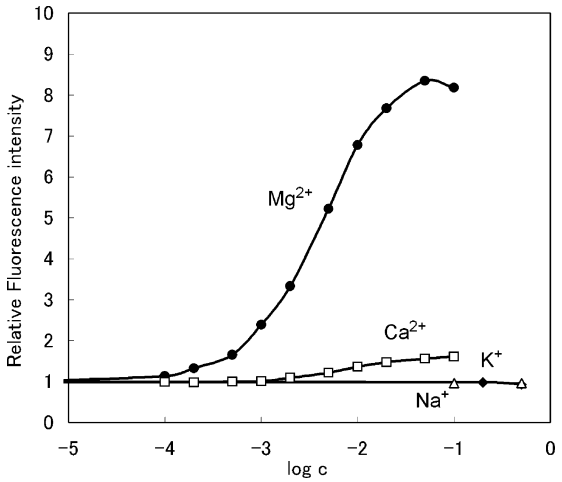

Figure 3. Fluorescence intensity at 524 nm (arbitrary units, excitation at 490 or 504 nm) of KMG-104 (5 μM) in the presence of different cations in concentrations ranging from 0.1 to 100 mM (□, Ca^{2+}; ●, Mg^{2+}) and from 100 to 1000 mM (△, Na^+; ◆, K^+). All spectra were measured at pH 7.20 (50 mM HEPES buffer, 130 mM KCl, 20 mM NaCl).

represented by eq 2 for KMG-103 and KMG-104 ($R > 0.99$). In the case of KMG-101, a Benesi−Hildebrand plot was used, since the maximum fluorescence value could not be determined. A 1:1 complexation between Mg^{2+} and each fluorescent probe was assumed.

KMG-103 and -104 had dissociation constants around 2 mM (Table 2), being much lower than for KMG-101 ($K_{d,Mg^{2+}} = 100$ mM). This observation demonstrates the effect of the electron-donating N-substituent near the charged β-diketone binding site, which effectively increased the Mg^{2+} affinity.

KMG-101 has a lower affinity for Mg^{2+}, while KMG-103 and -104 have higher ones, making the latter more suitable for the intracellular Mg^{2+} measurements.

Selectivity toward Interfering Cations. The selectivity toward biologically interfering ions is shown in Figure 3. The dissociation constants $K_{d,Ca^{2+}}$ and the fluorescence enhancement factors (FEFs) for Ca^{2+} are summarized in Table 2.

No response toward alkali metals (Na^+, K^+) was observed for all compounds in the KMG-100 series. Of special relevance for characterizing Mg^{2+} probes is the Ca^{2+} selectivity, since intracellular Ca^{2+} concentration changes are large. All the members of the KMG-100 series exhibited a 1.5−3-fold complexation selectivity for Mg^{2+} over Ca^{2+} caused by the charged β-diketone binding site which forms a size-fitting cavity for Mg^{2+}. Furthermore, the Ca^{2+}-induced fluorescence enhancement was more than 2-fold lower than for Mg^{2+}, because of the lower surface electron density of the Ca^{2+} ion. Consequently, KMG-103 and -104 showed nearly 10-fold higher sensitivity toward Mg^{2+} in the fluorescence response compared to Ca^{2+}. Ca^{2+} response was observed at concentrations above 1 mM. Nevertheless, this concentration is much higher than the one normally found at the cell level.

The sensitivity of the magnesium fluorescent probes KMG-103 and KMG-104 toward variations in the sample pH is shown in Figure 4. Although the fluorescence intensity of KMG-101 changed at pH values below 7 (data not shown), KMG-103 and -104 showed only a weak response toward pH in the range of 6.0−8.5, while the biologically relevant pH range is 6.0−7.6. These differences in the response behavior can be attributed to the halogen substitution in the fluorescein moiety. As a

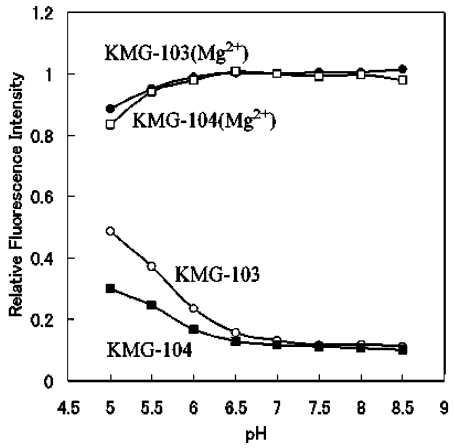

Figure 4. Effect of the pH on the fluorescence intensity of KMG-103 and KMG-104: ○, KMG-103 (ion-free); ●, KMG-103 (100 mM Mg^{2+}); ■, KMG-104 (ion-free); □, KMG-104 (100 mM Mg^{2+}); [probe] = 5 μM for all cases; pH 5−6.5 (50 mM MES, 100 mM KCl), pH 7−8.5 (50 mM HEPES, 100 mM KCl). Excitation/emission wavelength (nm): KMG-103 (517/533), KMG-104 (490/524).

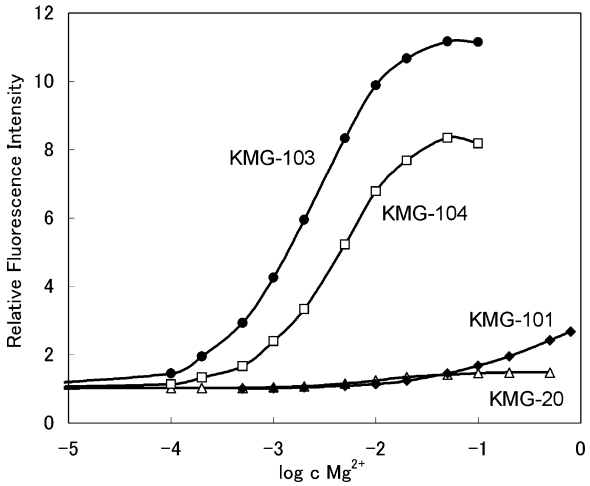

Figure 5. Comparison of the normalized fluorescence intensities of KMG-20, -101, -103, and -104 in the presence of Mg^{2+} ranging from 0.1 to 100 mM (●, KMG-103; □, KMG-104) and from 0.1 to 800 mM (△, KMG-20; ◆, KMG-101). These spectra were measured at pH 7.20 (50 mM HEPES buffer, 130 mM KCl, 20 mM NaCl). [KMG-20] = 10 μM, and [KMG-101] = [KMG-103] = [KMG-104] = 5 μM. Excitation/emission wavelength (nm): KMG-20 (448/490), KMG-101 (488/516), KMG-103 (517/533), KMG-104 (490/524).

consequence, KMG-103 and -104 are pH-insensitive under the conditions normally found in an intracellular environment. Hence, it can be concluded that pH, Na^+, K^+, and Ca^{2+} do not interfere with the intracellular Mg^{2+} concentration measurements using the newly developed magnesium probes KMG-103 and -104.

Comparison of Probes in the KMG Series. The interference by other relevant cations (except pH) is negligible for all the indicators; therefore, the discussion of their differences is focused on the sensitivity toward Mg^{2+} as indicated by the dissociation constant K_d and the FEF.

In Figure 5, the response of the magnesium probes belonging to the KMG-100 series is compared to that of the previously reported KMG-20.[13] The fluorescent enhancement for KMG-20 is rather low (about 1.5-fold), since its response mechanism is based on an ICT (internal charge transfer) type mechanism.

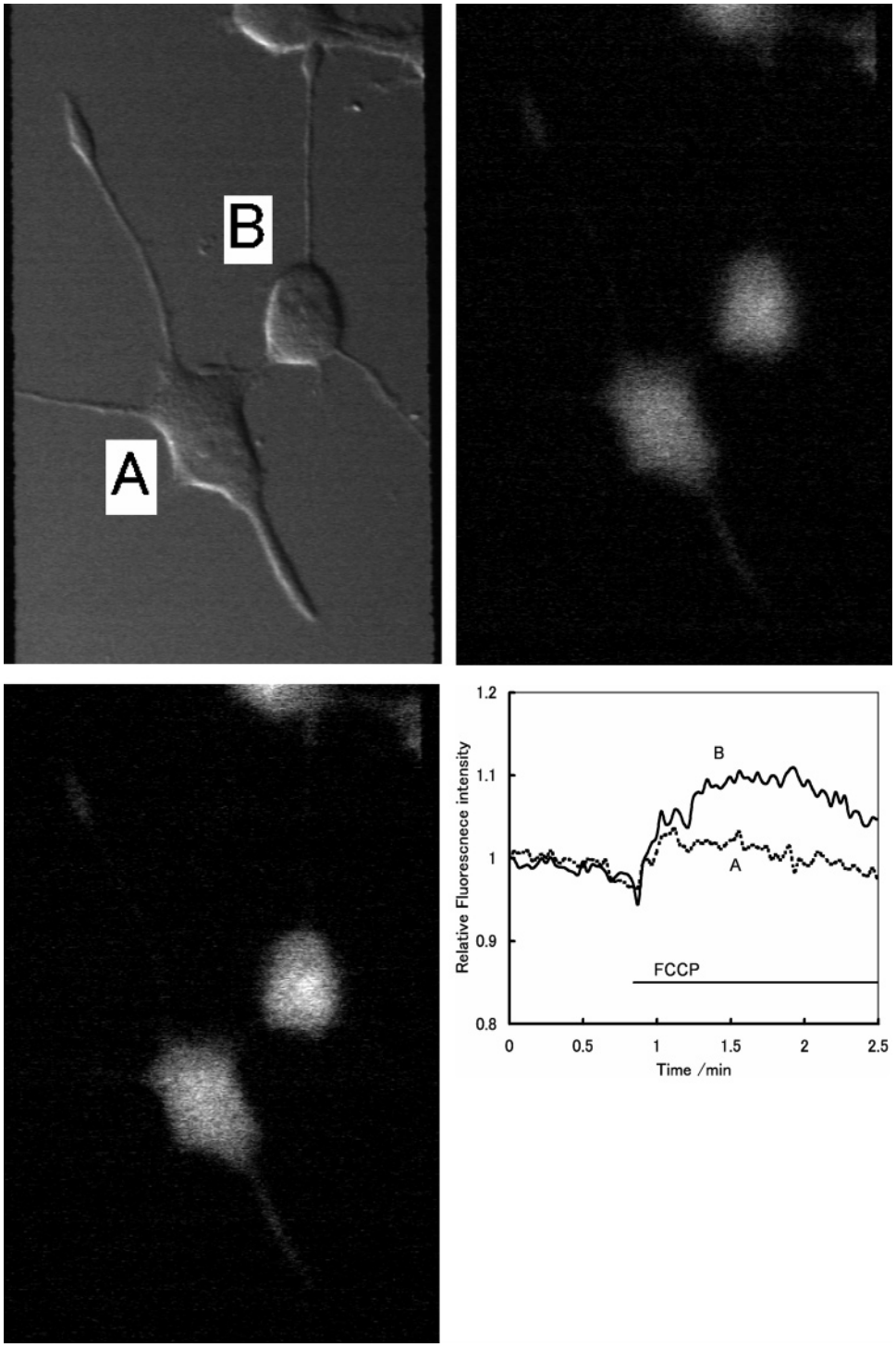

Figure 6. (a, top left) Differential interference contrast (DIC) image, (b, top right; c, bottom left) Fluorescent images of PC-12 cells loaded with KMG-104AM (image taken (b) before and (c) after application of FCCP). (d, bottom right) Time course of fluorescence intensity in cytosol: cell A (dashed line), cell B (solid line). FCCP was applied at $t = 50$ s, and the resulting fluorescence increase was observed.

The dynamic ranges of both KMG-20 and KMG-101 are not suitable for intracellular conditions. KMG-103 and -104 showed a better response (nearly 10-fold enhancement) and a dynamic range suitable for biological Mg^{2+} concentrations (0.1−6 mM).

Practical Application of KMG-104 to Intracellular Mg^{2+} Measurement. It was demonstrated that the indicator KMG-104, having a high affinity, favorable photophysical properties, and the ability to be excited with the 488 nm line of the Ar^+ laser, is suitable for cell imaging. To simplify its cell loading, the derivative KMG-104AM was synthesized.

KMG-104AM was easily loaded into PC12 cells by incubation, and the cells were observed under a fluorescent microscope. Figure 6a shows a differential interference contrast image.

The photobleaching and sequestration lifetimes of KMG-104 were measured under these conditions, and the half-life was found to be 28 min for photobleaching and 30 min for the

sequestrations. Therefore, both effects are negligible for detecting short-time signals in cells.

Additionally, the intracellular resting Mg^{2+} concentration was determined using a modified literature method.[24] The resulting Mg^{2+} concentration was 0.90 ± 0.16 mM.

The possibility of using KMG-104 to detect intracellular Mg^{2+} signals was evaluated. After the application of FCCP, acting as a mitochondria uncoupler, an immediate fluorescence intensity increase was observed in cells A and B (Figure 6b,c). After this treatment, the fluorescence intensity gradually decreased back to the initial base level (Figure 6d).

This observed result is consistent with previous reports,[20] and is interpreted as a magnesium ion concentration increase resulting from ATP hydrolysis and/or a Mg^{2+} efflux from mitochondria. After the FCCP-induced Mg^{2+} increase, the magnesium ion concentration gradually decreased to the base level, due to a Mg^{2+}/Na^{+} exchanger located at the cell membrane.[4]

Intracellular 3D Mg^{2+} Imaging. The λ_{max} value of KMG-104 is found close to 488 nm, and the probe can be excited with the commonly used Ar^{+} laser for the confocal microscope. KMG-104AM was applied to PC12 cells, and the 3-D images of the intracellular Mg^{2+} distribution were successfully taken. The surface and topographic images are shown in Figure 7.

Fluorescence was observed all over the cell, with bright areas in the nucleus and the brightest range in the nucleolia-like regions. The reason for this phenomenon may be the localization of KMG-104 in these specific areas of the cell and/or the heterogeneous intracellular distribution of the magnesium ions.

It was demonstrated that KMG-104 allows the 3-D imaging of the intracellular magnesium concentration, and is capable of measuring the heterogeneous distribution[21] of magnesium ions in the cytosol.

Conclusion

The novel magnesium fluorescent probes KMG-101, -103, and -104 are characterized by having a strong PET-type fluorescent enhancement upon magnesium binding. They feature a high specificity for Mg^{2+} cations and are suitable for excitation by the Ar^{+} laser 488 nm line, commonly used in fluorescence microscopy. In addition, KMG-103 and -104 have suitable dynamic ranges for intracellular applications ($K_{d,Mg^{2+}} = 2$ mM). Their detection contrast at low magnesium levels is nearly 50-fold higher than for the previously reported probe KMG-20.

(24) Sharikabad, M. N.; Østbye, K. M.; Brørs, O. *Am. J. Physiol.: Heart Circ. Physiol.* **2001**, *281*, H2113−H2123.

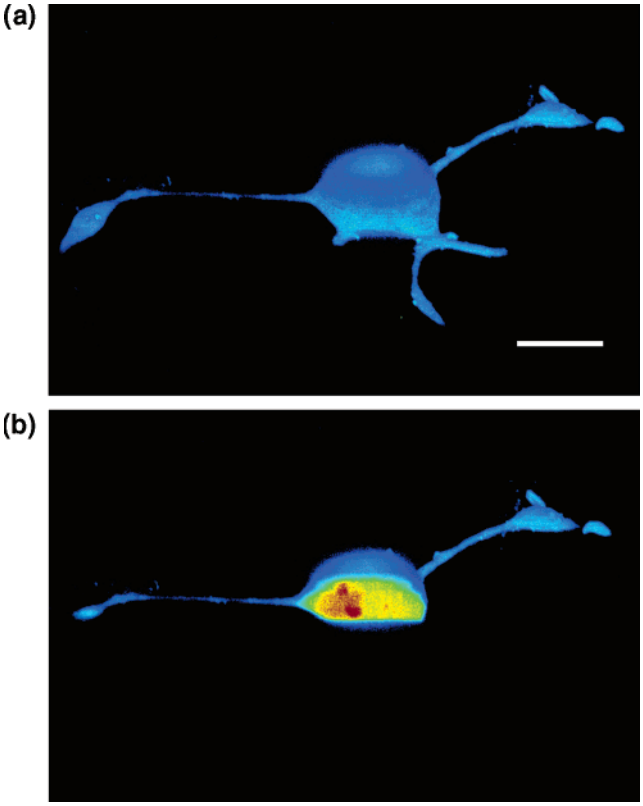

Figure 7. (a) Surface and (b) topographic images of a PC12 cell loaded with KMG-104AM (10 μM) observed using a confocal microscope. Bright fluorescence is observed in nucleolia-like regions.

By cell loading in the form of the acetoxymethyl derivative KMG-104AM, the probe can easily be applied to intracellular imaging.

The 3D images showed bright fluorescence in the nucleolia regions, suggesting that KMG-104 may be used to investigate the role of intracellular magnesium. These indicators could also be used for magnesium detection in blood or serum because of their high Mg^{2+}selectivity and sensitivity.

At present, KMG-103 and -104 are the most suitable Mg^{2+} fluorescent probes for biologists who want to investigate intracellular magnesium concentration dynamics especially using confocal microscopy.

Supporting Information Available: ^{1}H NMR chart of KMG-104. This material is available free of charge via the Internet at http://www.pubs.acs.org.

JA049624L